

Accepted Manuscript

Model-based analysis of the autonomic response to head-up tilt testing in Brugada syndrome

Mireia Calvo, Virginie Le Rolle, Daniel Romero, Nathalie Béhar, Pedro Gomis, Philippe Mabo, Alfredo Hernández



PII: S0010-4825(18)30300-7

DOI: [10.1016/j.combiomed.2018.10.007](https://doi.org/10.1016/j.combiomed.2018.10.007)

Reference: CBM 3102

To appear in: *Computers in Biology and Medicine*

Received Date: 4 July 2018

Revised Date: 13 September 2018

Accepted Date: 8 October 2018

Please cite this article as: M. Calvo, V. Le Rolle, D. Romero, N. Béhar, P. Gomis, P. Mabo, A. Hernández, Model-based analysis of the autonomic response to head-up tilt testing in Brugada syndrome, *Computers in Biology and Medicine* (2018), doi: <https://doi.org/10.1016/j.combiomed.2018.10.007>.

This is a PDF file of an unedited manuscript that has been accepted for publication. As a service to our customers we are providing this early version of the manuscript. The manuscript will undergo copyediting, typesetting, and review of the resulting proof before it is published in its final form. Please note that during the production process errors may be discovered which could affect the content, and all legal disclaimers that apply to the journal pertain.

Model-based Analysis of the Autonomic Response to Head-up Tilt Testing in Brugada Syndrome

Mireia Calvo^a, Virginie Le Rolle^{a,*}, Daniel Romero^a, Nathalie Béhar^a, Pedro Gomis^{b,c},
Philippe Mabo^a, Alfredo Hernández^a

^a*Univ Rennes, CHU Rennes, Inserm, LTSI - UMR 1099, Rennes, F-35000, France*

^b*ESAI, EEBE, Universitat Politècnica de Catalunya, Barcelona, E-08028, Spain*

^c*CIBER of Bioengineering, Biomaterials and Nanomedicine, Zaragoza, E-50018, Spain*

Abstract

The etiology of Brugada syndrome (BS) is complex and multifactorial, making risk stratification in this population a major challenge. Since changes in the autonomic modulation of these patients are commonly related to arrhythmic events, we analyze in this work whether the response to head-up tilt (HUT) testing on this population may provide useful, complementary information for risk stratification. In order to perform this analysis, a coupled physiological model integrating the cardiac electrical activity, the cardiovascular system and the baroreceptors reflex control of the autonomic function, in response to HUT is proposed. A sensitivity analysis was performed, based on a screening method, evidencing the influence of cardiovascular parameters on blood pressure and of baroreflex regulation on heart rate. The most sensitive parameters have been identified on a set of 20 subjects (8 controls and 12 BS patients), so as to assess subject-specific model parameters. According to the results, controls showed an increased sympathetic modulation after tilting, as well as a reduced left ventricular contractility was observed in symptomatic, with respect to asymptomatic BS patients. These results provide new insights regarding the autonomic mechanisms regulating the cardiovascular system in BS which might be used as a complementary source of information, along with classical electrophysiological

*Corresponding author (Tel: +33 2 23 23 62 20; Fax: +33 2 23 23 69 17)
Email address: virginie.lerolle@univ-rennes1.fr (Virginie Le Rolle)

parameters, for BS risk stratification.

Keywords: Autonomic nervous system, Brugada syndrome, physiological model, sensitivity analysis, parameter identification

1. Introduction

Brugada syndrome (BS) is a genetic disease characterized by a distinct ST-segment elevation on the electrocardiogram of right precordial leads, associated with an elevated risk for sudden cardiac death (SCD) due to ventricular fibrillation (VF) in absence of structural cardiopathies [1].

Major cardiac events in this population typically occur at rest and mainly at night, thus being frequently assumed that an increased parasympathetic activity may play a determinant role in the pathophysiology, arrhythmogenesis and prognosis of the disease [2, 3]. Moreover, some studies on cardiac autonomic nervous system (ANS) analyzed by positron emission tomography have reported a sympathetic autonomic dysfunction in BS [3, 4, 5]. However, despite the grounds for belief that autonomic assessment may provide valuable information for the prediction of VF in BS, it remains unclear which are the most suitable autonomic tests and indicators that may provide useful information to identify those patients at high risk.

Most previous investigations concerning the autonomic function in BS are based on long-term measurements, being time-consuming and leading to contradictory results [6, 7, 8, 9, 10, 11, 12, 13]. However, autonomic assessment can be improved by stimulating the ANS through standardized autonomic maneuvers such as exercise [14, 15] or the head-up tilt (HUT) test. As a matter of fact, the cardiovascular response to upright posture has been widely evaluated by means of computational models and clinical trials [16, 17, 18, 19]. Its main hemodynamic effect is the redistribution of blood volume to the lower part of the body, causing a decrease in both central venous return and ventricular filling pressures, as well as in stroke volume [20]. Consequently, cardiovascular regulatory mechanisms such as the arterial and cardiopulmonary baroreceptors

stimulate a reflex increase in sympathetic activity and a vagal inhibition, inducing an increase in heart rate, peripheral vascular resistance, venous tone and cardiac contractility [21].

30 Although several time- and frequency-domain indicators have been extensively used in clinical practice to estimate autonomic modulation [22], they sometimes fail to represent this response, even in healthy subjects [23, 24], but also in our previous works on BS patients [15, 25]. Since computational models also describe interactions between the ANS and the cardiovascular system
35 (CVS), we believe that a model-based approach could be a step forward towards the interpretation of the autonomic function in BS.

Therefore, this work proposes a global model-based strategy for the analysis of the cardiovascular response to HUT, including: i) the introduction of a CVS model and its short-term autonomic regulation in response to HUT testing, ii) a
40 sensitivity analysis, and iii) the development of patient-specific models for both healthy and Brugada subjects.

2. Methods

2.1. Global model-based strategy

In order to design a model-based subject-specific estimation of cardiovascular
45 dynamics and its autonomic modulation in response to HUT testing, we applied the following three main steps represented in Fig. 1 and explained in more detail in the following sections:

- Construction of the computational model capturing CVS and ANS interactions.
- 50 • Selection of the most influential parameters on model outputs, by means of a sensitivity analysis.
- Design of subject-specific cardiovascular models by estimating selected parameters, based on experimental data.

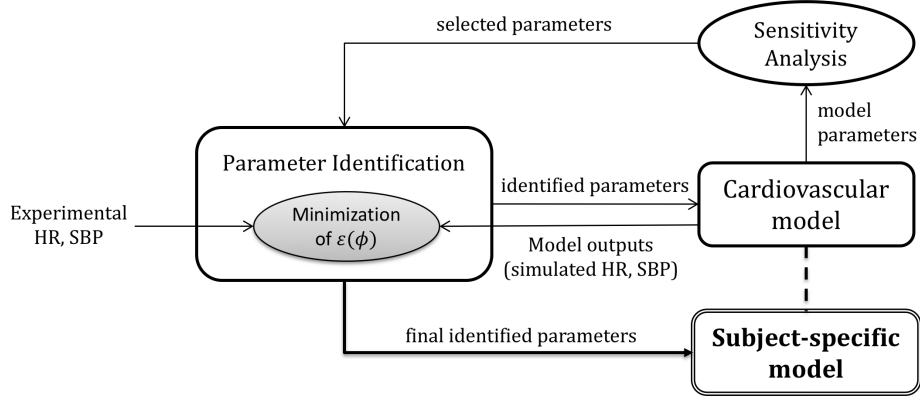


Figure 1: Diagram of the global model-based approach. After the construction of a cardiovascular model, we applied a sensitivity analysis to identify those model parameters leading to the highest effects on model outputs: simulated heart rate (HR) and systolic blood pressure (SBP). The selected parameters were then optimized for each subject, based on the minimization of the error function $\epsilon(\phi)$, proportional to the difference between simulated and experimental HR and SBP signals. Subject-specific models were finally constructed with those final identified parameters, leading to the lowest errors.

2.2. Computational model

55 The proposed cardiovascular model is based in our previous works in the field [26, 27, 28, 29, 30]. All simulations were performed using a multi-formalism modeling and simulation library (M2SL 1.8.4) developed by our team. Details regarding the simulation methods in this library can be found in [28, 31]. The model consists in 4 coupled submodels representing: 1) the cardiac electrical
60 system (CES), 2) the cardiovascular system (CVS), 3) the baroreceptors reflex system (BRS), and 4) the head-up tilt test (HUTT).

2.2.1. Cardiac electrical system

The cardiac conduction system was adapted from [32]. The CES is defined as a set of interconnected cellular automata, each one representing the electrical
65 activation of tissue-level cardiac structures: the sinoatrial node (SAN), the left atrium (LA), the atrioventricular node (AVN), the upper bundle of His (UBH),

the lower bundle of His (LBH), left and right bundle branches (LBB and RBB), and left and right ventricles (LV and RV). The automaton state periodically changes among four depolarization/repolarization phases: slow diastolic depolarization (SDD) for nodal automata or IDLE for myocardial automata, upstroke
70 depolarization period (UDP), absolute refractory period (ARP) and relative refractory period (RRP). The slope of the SDD phase in SAN depends on the HR that results from the BRS model, as well as the electrical activations of LV and RV are connected to the CVS model ventricular contractions. Moreover, since
75 BS patients present ECG patterns of right bundle branch block, we adjusted the RBB automata of these patients based on their baseline QRS durations. Further details on the CES model implementation can be found in [32].

2.2.2. Cardiovascular system

In order to represent the hemodynamic effects of postural changes, we adapted
80 the cardiovascular model defined in [33, 34, 35, 27]. As illustrated in Fig. 2 and described in previous models of our team [18], we integrated both pulmonary and systemic circulations, dividing the latter into three parallel vascular branches: 1) head or higher parts of the body, 2) hydrostatic indifference point (HIP) or heart level, and 3) legs or lower parts of the body. This subdivision allows for the
85 representation of differences on the impact of autonomic regulatory mechanisms at each branch, based on its distance from the HIP.

For each ventricular chamber ($m \in \{LV, RV\}$), volumes (V_m) are computed from the integral of their respective net flows. Blood pressure (P_m) is then calculated from its volume using two pressure-volume relationships associated
90 with systole and diastole, respectively, and a periodic function ($e_m(t)$) drives the transition between the systolic ($P_{es,m}$) and diastolic ($P_{ed,m}$) relationships as follows:

$$P_m(V, t) = e_m(t)P_{es,m}(V_m) + (1 - e_m(t))P_{ed,m}(V_m). \quad (1)$$

The systolic elastance (E_m) and the dead volume ($V_{d,m}$), or volume at zero end-systolic pressure, represent the slope and intercept of the linear relationship

95 between pressure and volume during systole. During diastole, this relationship is non-linear and described by a gradient ($P0_m$), curvature (λ_m) and volume at zero pressure ($V0_m$).

$$P_{es,m}(V_m) = E_m \cdot (V_m - Vd_m), \quad (2)$$

$$P_{ed,m}(V_m) = P0_m \cdot (\exp(\lambda_m(V_m - V0_m)) - 1). \quad (3)$$

The diastolic and systolic dynamics are driven by a Gaussian function (Eq.4) described by its amplitude (A), width (B) and center (C). The onset of the cardiac cycle, denoted t_m , is determined by the activation instant of the corresponding chamber in the cardiac electrical model presented in the previous section.

$$e_m(t) = A \cdot \exp(-B \cdot ((t - t_m) - C)^2). \quad (4)$$

Based on the minimal cardiovascular model described by Smith et al. [33], atria were omitted since they minimally contribute to main cardiac trends. However, ventricular interactions were represented by coupling ventricles through the septum. Being V_{spt} the septum volume, the model defines left and right ventricle free wall volumes as:

$$V_{LVf} = V_{LV} - V_{spt}, \quad (5)$$

$$V_{RVf} = V_{RV} + V_{spt}. \quad (6)$$

105 Pressures on the systemic and pulmonary circulations are calculated as a linear relationship of their volume and vascular elastance, following eq. 2. These pressures are then used to calculate flows between chambers as $Q = \frac{\Delta P}{R}$, where ΔP is the pressure gradient of two chambers and R is the corresponding vascular resistance connecting them. Fig. 2 represents those parameters involved in the implemented cardiovascular model.

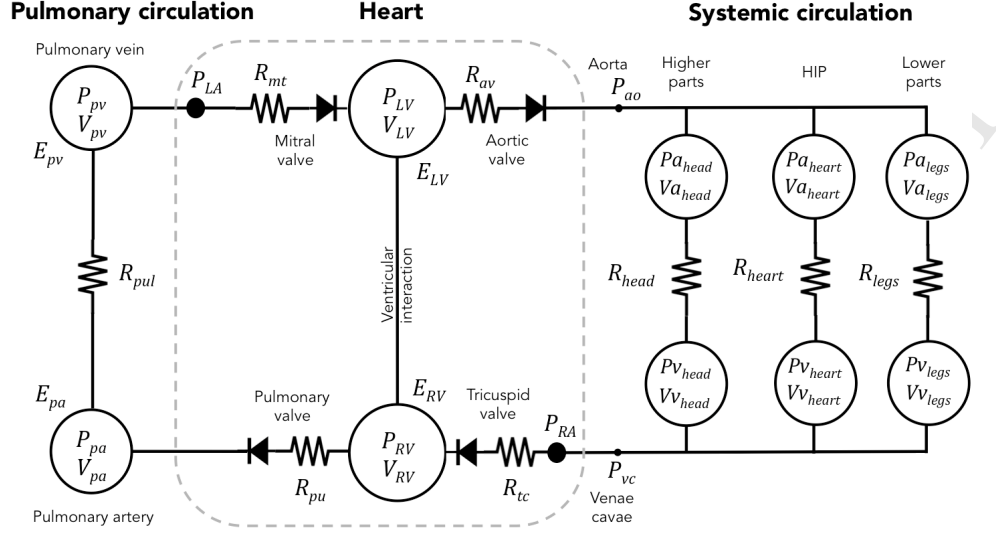


Figure 2: Schematic representation of the cardiovascular model integrating the cardiac mechanical activity, the pulmonary circulation and a three-branch systemic circulation. E: elastance; R: resistance; P: pressure; V: volume; pul: pulmonary; pv: pulmonary vein; pa: pulmonary artery; pu:pulmonary valve; av: aortic valve; ao: aorta; vc: venae cavae; LA: left atrium; LV: left ventricle; RA: right atrium; RV: right ventricle.

2.2.3. Baroreflex model

We modeled sympathetic and parasympathetic efferent responses to arterial blood pressure regulation based on a widely used approach [18, 36]. Since arterial baroreceptors are located above the heart level, the input pressure for the BRS model came from the higher compartment of the systemic circulation.

Baroreceptors dynamics are represented in Fig. 3 by a first-order transfer function, whose gain and time constant are denoted as K_B and T_B . Then, five different efferent pathways control heart rate, systemic resistance, venous volume and cardiac contractility; by means of a normalization function, a delay and a first-order filter. The normalization function is represented by the following sigmoidal input-output relationship:

$$F x(t) = a_x + \frac{b_x}{\exp[\lambda_x(P_B(t) - M_x)] + 1}, \quad (7)$$

where P_B is the arterial baroreceptors pressure; a_x , b_x , λ_x and M_x permit to adjust the sigmoid; and $x \in \{V, S, R, VV, C\}$ refers to vagal heart rate, sympathetic heart rate, systemic resistance, venous volume and cardiac contractility control, respectively. In Fig. 3, resistance, venous volume and cardiac contractility modulations are compactly represented as θ . The same notation is used for gains (K_x), delays (D_x) and time constants (T_x) describing first-order transfer functions:

$$\Delta x = K_x \frac{\exp[-D_x s]}{1 + T_x s}. \quad (8)$$

For each regulated variable, Δx is then added to a baseline response. In chronotropic modulation, though, HR is the result of adding both vagal (V) and sympathetic (S) contributions to an intrinsic heart rate ($HR0$).

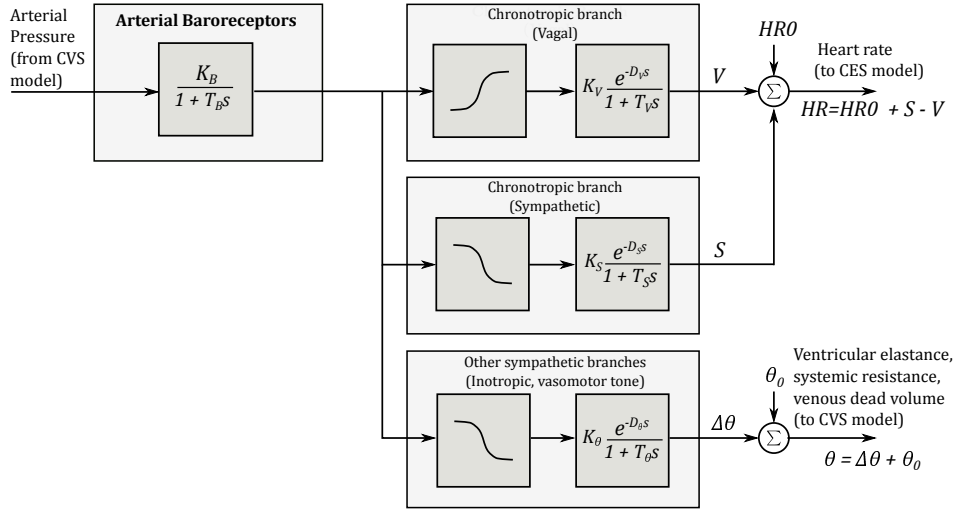


Figure 3: Diagram of the implemented BRS model. From the arterial pressure registered at the higher systemic circulation, the baroreflex system regulates heart rate, peripheral resistance, venous volume and heart contractility.

2.2.4. HUT test model

Upright posture stimulates blood pressure variations in different body parts. As in [18, 19], we implemented the effect of gravity at each systemic branch,

135 based on its distance to HIP. Being Pa_k the arterial pressure in supine rest for each systemic branch where $k \in \{head, heart, legs\}$, the arterial pressure at each compartment P_k during tilting is described as:

$$P_k = \begin{cases} Pa_k + Pg_k \cdot \sin(\alpha(t)), & t_0 < t < t_{tilt}, \\ Pa_k + Pg_k \cdot \sin(\alpha_{max}), & t > t_0 + t_{tilt}. \end{cases} \quad (9)$$

Where $\alpha(t)$ is the tilt table angle, which goes from 0 to α_{max} , t_0 is the table inclination onset, t_{tilt} is the time to α_{max} and Pg_k is the pressure due to gravity at each branch, defined as:

$$Pg_k = \rho \cdot g \cdot h_k, \quad (10)$$

where ρ is the fluid density, g the gravitational constant and h_k the mean distance between the systemic branch and HIP. Therefore, $Pg_{heart} = 0$, $Pg_{head} = -20$ mmHg, based on [18], and Pg_{legs} was identified for each subject.

2.3. Sensitivity analysis

145 In order to identify the most influential model parameters on simulated outputs, we performed a sensitivity analysis, based on the screening method of Morris [37], on 62 parameters coming from the BRS and CVS submodels. Supplementary Tables I and II include a brief description of these parameters as well as the analyzed intervals, based on physiological ranges reported in the literature on both pathological and healthy conditions [18, 19, 36].

This method not only evaluates non-linearities and interactions between parameters, but it also provides an estimation of each variable's significance with limited computational costs. Hence, it permits excluding unimportant model parameters so as to reduce the dimensionality of subsequent analyses.

155 It consists in the generation of r random trajectories through the parameter space; each trajectory being associated with an estimation of the Elementary

Effects EE_{ij} of a parameter x_i on output y_j :

$$EE_{ij} = \left| \frac{y_j(x_1, \dots, x_i + \Delta, \dots, x_k) - y_j(x_1, \dots, x_i, \dots, x_k)}{\Delta} \right|, \quad (11)$$

where $\Delta = \frac{p}{2^{(p-1)}}$, p is defined as the number of levels dividing the parameter space and y_j stands for each analyzed model output expressed as a function of k parameters ($y_j = f(x_1, \dots, x_i, \dots, x_k)$).
 160

For each combination of parameter x_i and output y_j , the mean μ_{ij}^* and standard deviation σ_{ij} of the r elementary effects are calculated. A large value of μ_{ij}^* indicates a significant effect of x_i on y_j , whereas a large σ_{ij} value is related to either non-linear or strongly interacting variables. Thereby, parameters can be classified as being negligible (low μ_{ij}^* and σ_{ij}), linear (non-zero $\mu_{ij}^* > \sigma_{ij}$) and non-linear or presenting strong interactions with other parameters (non-zero $\mu_{ij}^* \leq \sigma_{ij}$).
 165

We computed these effects on the mean heart rate (HR) resulting from the BRS submodel and on the mean systolic blood pressure (SBP) detected at the lower systemic compartment (CVS submodel). Moreover, we divided the evaluation in supine and upright postures since cardiac signals present different behaviors for each postural status: $y \in \{HR_{supine}, SBP_{supine}, HR_{tilt}, SBP_{tilt}\}$.
 170

In order to establish a global rank of importance among parameters, we calculated D_{ij} , defined as the Euclidean distance in the $\mu^* - \sigma$ plane, from the origin to each $(\mu_{ij}^*, \sigma_{ij})$ point:
 175

$$D_{ij} = \sqrt{(\mu_{ij}^*)^2 + \sigma_{ij}^2}, \quad (12)$$

being parameters with high sensitivities or strong interactions those presenting the highest values for D_{ij} .

2.4. Parameter identification

Based on sensitivity results, we selected a reduced group of parameters for subject-specific model identification. The optimization process consisted in the
 180

minimization of the error function ϵ , based on the comparison of simulation outputs and experimental signals acquired during HUT testing:

$$\epsilon(\phi) = \sum_{j=1}^4 \sum_{i=1}^{N_j} \left| \frac{Y_{sim,\phi}^j(i) - Y_{exp}^j(i)}{\max(Y_{exp}^j(i))} \right|^2. \quad (13)$$

$Y_{exp}^j(i)$ and $Y_{sim,\phi}^j(i)$ are the i^{th} experimental value and the i^{th} model output sample for the simulation of Y^j when using the set of parameters ϕ . Moreover, N_j indicates the number of samples for each output being compared and Y^j refers to HR and SBP signals for the whole test and only during the transition of table inclination: $Y \in \{SBP_{total}, SBP_{transition}, HR_{total}, HR_{transition}\}$. Note from eq. 13 that identification is based on both HR and SBP signals, and mainly on their transitory periods since they are accounted twice to ensure that errors in this segment are particularly penalized. Transitory periods in SBP and HR signals are specially relevant since they respectively reflect the cardiovascular and autonomic responses to postural change.

As in previous works of our team [29, 30], we identified the best set of parameters for each subject through an approach based on evolutionary algorithms (EA). These stochastic search methods are founded on theories of natural evolution, such as selection, crossover and mutation [38]. Being an individual the representation of an optimization solution (a parameter value set ϕ), we started with the initialization of 50 random individuals, each parameter value of the individual being randomly selected from a specified parameter space. By quantifying each individual error through equation 13, the population was continuously evolved to 30 generations, following four main steps:

1. Selection of parent individuals for combination, biased towards those providing the lowest errors.
2. According to a probability p_c , combination of parent individuals through crossover to generate new children. Then, with a probability p_m , modification of these individuals by means of mutations.
3. Error assessment in new individuals.
4. Replacement of individuals having the highest errors.

Model parameters estimated for each subject were then compared by means
 210 of Mann-Whitney U non-parametric tests, so as to identify statistically significant differences between healthy subjects and BS patients, as well as between symptomatic and asymptomatic patients.

The autonomic response to HUT testing was also assessed and compared
 between populations, by means of the vagal and sympathetic HR modulations.
 215 More specifically, the vagal (V) and sympathetic (S) chronotropic outputs of the BRS submodel were averaged for both supine and upright positions. Thus, being ΔS and ΔV , respectively, the mean sympathetic and vagal HR regulation differences between supine and upright positions, these variables were also compared among populations.

Finally, the difference between experimental (Y_{exp}) and the resulting simulated (Y_{sim}) signals was quantified in percentage as:

$$E_Y = \frac{1}{n} \sum_{i=1}^n \left| 100 \cdot \frac{Y_{sim}(i) - Y_{exp}(i)}{Y_{exp}(i)} \right|, \quad (14)$$

where $Y \in \{HR, SBP\}$ and n is the number of samples being compared.

2.5. Experimental protocol and data

HUT tests were performed on 8 healthy subjects and 12 BS patients (5
 225 were symptomatic), recruited at the University Hospital of Rennes, in France. Controls were healthy volunteers with no major cardiorespiratory pathologies diagnosed, non-smokers, asymptomatic and not taking cardioactive medication. BS patients were diagnosed according to current guidelines, when a coved ST-segment elevation (≥ 0.2 mV) was registered in at least one right precordial lead
 230 placed in the second, third or fourth intercostal space, either in the presence or absence of sodium channel blockers [1].

After approval by the ethical committee of the University Hospital of Rennes, all subjects provided written informed consent to participate in the study. Table 1 summarizes participants clinical baseline characteristics, including their
 235 mean HR, mean SBP and mean baroreflex sensitivity (BRS) in supine position, calculated as in [39, 17].

Table 1: Baseline characteristics of participants.

	Controls (n=8)	BS patients (n=12)	p-value
Age, years old	30.8 ± 5.7	50.1 ± 12.1	<0.001
Male sex, n (%)	8 (100%)	10 (83.3%)	0.266
Body weight, kg	71.5 ± 7.2	69.2 ± 11.8	0.756
Height, m	1.75 ± 0.06	1.74 ± 0.08	0.877
BMI, kg/m²	23.3 ± 1.5	22.8 ± 3.3	0.396
Mean HR, bpm	67.56 ± 7.40	63.23 ± 9.84	0.232
Mean SBP, mmHg	103.88 ± 20.27	113.99 ± 23.77	0.298
Mean BRS, ms/mmHg	14.45 ± 11.17	11.74 ± 10.12	0.512

Since no significant differences in gender, body weight, height, body mass index (BMI), HR, SBP or BRS were noted between groups (p -value>0.05), similar baseline characteristics were assumed between populations. However, the fact that BS patients were significantly older than controls may have a significant impact on autonomic function analysis.

Regarding BS patients, five presented documented symptoms of ventricular origin: cardiac arrest (60%) and syncope (40%). Three patients (2 were symptomatic) presented an SCN5A mutation (25%). An Implantable Cardioverter Defibrillator (ICD) had been placed in one asymptomatic patient, based on a positive EPS (Electrophysiological Study) test, whereas all symptomatic patients had ICDs implanted. Since no relevant cardiac events were noted during HUT testing, defibrillators caused no significant effects on recordings. Indeed, the incidence of ventricular fibrillation during HUT testing is extremely rare (0.04%) and has only been reported in the presence of pharmacological stimulation, in patients with either underdiagnosed underlying significant coronary artery disease, known structural heart disease, or apical hypertrophic cardiomyopathy [40, 41, 42, 43].

Participants underwent HUT tests in fasting conditions, between 8 a.m. and

255 10 a.m., in a quiet room with dim lights and no pharmacological provocation,
while non-invasive blood pressure and ECG recordings were acquired with the
Task Force monitor (CN Systems, Graz, Austria) at a sampling frequency of
210 100 Hz and 1000 Hz, respectively, according to the following protocol:

- Pre-tilt resting phase: 10 minutes in supine position.
- 260 • Tilting phase: 45 minutes at 60° of table (Sissel, Sautron, France) incli-
nation or until the test was positive.
- Post-tilt resting phase: 10 minutes in supine position.

A positive response to tilting was defined by a symptomatic decrease in heart
rate of 20% and/or in blood pressure of 30% with respect to baseline values.
265 Nevertheless, all analyzed HUT tests were negative.

The systolic blood pressure associated with each heartbeat was detected as
the maxima above a manually adjusted threshold and heart rate signals were
detected by means of a noise-robust wavelet-based method for QRS identifica-
tion and R-wave peak location [44]. In order to ease the comparison with model
270 simulations, experimental data were low-pass filtered at 0.04 Hz with a 4^{th} or-
der Butterworth filter applied in both forward and backward directions so as to
remove phase distortion. Moreover, since we were particularly interested in the
response induced by changing from supine to upright posture, cardiac signals
were only analyzed for 2.5 minutes before and after tilting onset.

275 **3. Results**

3.1. Sensitivity analysis

As in [29], we applied the screening method of Morris with a grid of $p = 20$
and we calculated $r = 5 \cdot k = 310$ elementary effects, performing a total of
almost 20,000 simulations. Fig. 4 represents sensitivity results on the mean SBP
280 and HR signals for supine and tilting phases, only labeling the most relevant
parameters in order to improve readability.

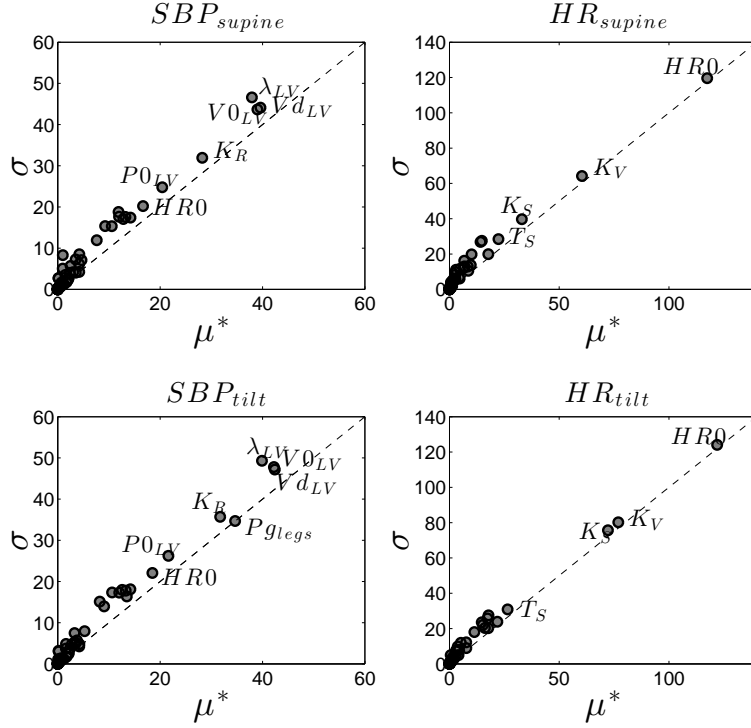


Figure 4: Absolute mean (μ^*) and standard deviation (σ) of the elementary effects for the mean SBP and HR, during supine and tilting phases. Only the most significant parameters are labeled: λ_{LV} (LV end-diastolic exponent), Vd_{LV} (LV volume at zero end-systolic pressure), $V0_{LV}$ (LV volume at zero end-diastolic pressure), K_R (gain for peripheral resistance modulation), $P0_{LV}$ (intrinsic LV pressure), $HR0$ (intrinsic heart rate), K_V (gain for vagal HR modulation), K_S (gain for sympathetic HR modulation), T_S (sympathetic time constant), and Pg_{legs} (pressure due to gravity at lower systemic compartment).

The general distribution of model parameters in the $\mu^* - \sigma$ space indicates effects on HR and SBP that are either non-linear or caused by the interaction with other parameters. Although some of them are close to the $\mu^* = \sigma$ reference line, Pg_{legs} was the most linearly related parameter to SBP_{tilt} . Nevertheless, many parameters showed a significant effect on the analyzed outputs. In order to identify those variables having the highest sensitivities or the strongest interactions, Fig. 5 displays the 15 most influential parameters on each analyzed

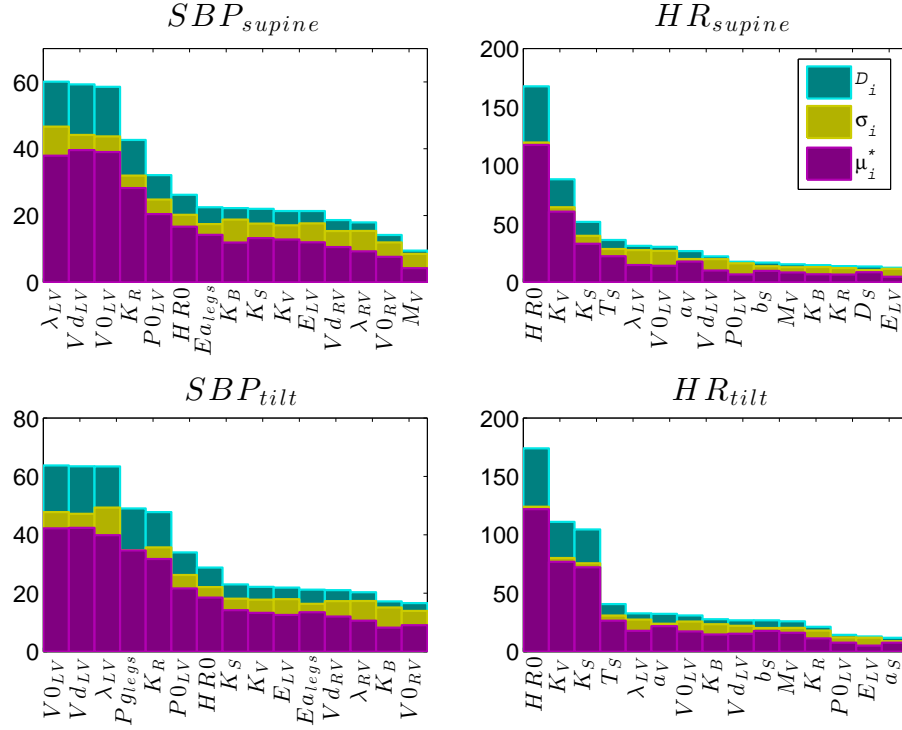


Figure 5: Most influential parameters on HR and SBP in supine and upright postures, based on the Morris sensitivity distance D_i (green bars). For each parameter, the absolute mean μ_i^* (purple bars) and the standard deviation σ_i (yellow bars) of the elementary effects are also displayed.

output based on their D_i index, represented along with their μ_i^* and σ_i values.

290 Similar results were obtained for supine and upright postures. Regarding SBP, the main difference concerned Pg_{legs} , being negligible in supine rest but turning into a significant parameter during tilting. Concerning HR, the most influential variables in supine rest remained the same during tilting. However, K_S gained importance with respect to supine rest, due to the sympathetic activation
 295 caused by postural change.

On one hand, SBP showed a significant dependence on λ_{LV} , $V0_{LV}$ and Vd_{LV} . K_R , $P0_{LV}$ and $HR0$ also led to high D_i values. Although the highest sensitivities were found for variables accounting for diastolic LV dynamics, the

effect of some RV variables, such as λ_{RV} , $V0_{RV}$ and Vd_{RV} , was still consider-
300 able. Indeed, the model defines that RV parameters can modulate LV through
the septum wall, the pericardium and the closed-loop circulation. This may
be relevant in BS, where patients present ECG patterns of right bundle branch
block (RBBB).

On the other hand, HR was mostly modulated by $HR0$, K_V and K_S . The
305 most relevant parameter was the intrinsic heart rate $HR0$, presenting an almost
linear effect on the output. Baroreflex gains modulating the sympathetic and
parasympathetic chronotropic branches were also significant, mostly in upright
position. Furthermore, since blood pressure and heart rhythm are closely con-
nected through the baroreflex arc, SBP was also significantly affected by these
310 autonomic variables.

Then, based on sensitivity analysis results and visual inspection, we se-
lected a reduced group of model parameters to be identified in a subject-specific
manner. Although $HR0$ demonstrated high sensitivities, in order to reduce
computational cost by reducing dimensionality, we did not include this param-
315 eter in the identification process. Instead, $HR0$ was simply estimated for each
participant as the mean HR in supine position. Likewise, we estimated all nor-
malization centers in the BRS submodel (M_V , M_S , M_R , M_C and M_{VV}) as the
mean SBP in supine rest, and we only identified one LV volume at zero-pressure
by assuming $V0_{LV} = Vd_{LV}$.

320 Together with Vd_{LV} , we also chose λ_{LV} , K_S and K_V as parameters to be
identified for each subject, since they showed the significantly highest sensitiv-
ities. Then, due to their non-negligible importance in sensitivity results, λ_{RV}
and K_R were also added to the identification process, in order to study varia-
tions induced by HUT testing in the right ventricle and in peripheral resistance.
325 Although K_C did not demonstrate a particularly high sensitivity, we included
this variable to analyze group differences in the baroreflex gain regulating in-
otropism. Moreover, since Pg_{legs} demonstrated a rather linear effect on SBP_{tilt} ,
we also included this parameter in the estimation step. Finally, since we experi-
mentally remarked that better estimations of the oscillations in HR and/or SBP

330 caused by postural changes were obtained by identifying the sympathetic and vagal time constants, we added T_S and T_V estimations. Similarly, higher and lower systemic time constants (τ_{head} and τ_{legs}) were included to better estimate the progressive adaptation of systemic circulation to postural changes. Table 2 specifies those variables retained for subject-specific parameter estimations.

Table 2: Parameters selected for identification. CVS: cardiovascular system; BRS: baroreflex system.

	Parameter description	Submodel
λ_{LV}	LV end-diastolic exponent	CVS
Vd_{LV}	LV volume at zero end-systolic pressure	CVS
λ_{RV}	RV end-diastolic exponent	CVS
K_S	Gain for sympathetic HR modulation	BRS
K_V	Gain for vagal HR modulation	BRS
K_R	Gain for peripheral resistance modulation	BRS
K_C	Gain for contractility modulation	BRS
Pg_{legs}	Pressure due to gravity at lower systemic compartment	CVS
T_S	Sympathetic time constant	BRS
T_V	Vagal time constant	BRS
τ_{head}	Higher systemic compartment time constant	BRS
τ_{legs}	Lower systemic compartment time constant	BRS

335 3.2. Parameter identification

Based on visual inspection and resulting errors for the entire cohort ($E_{SBP} = 2.90 \pm 1.63$ %; $E_{HR} = 3.39 \pm 1.00$ %), we noted an acceptable agreement between observed and estimated signals. Fig. 6 shows the average experimental and simulated SBP and HR signals for each study group, together with their mean and standard deviation errors. Moreover, the percentage errors of each subject are provided as supplementary material (Table III).

340 Although an acceptable global fit can already be noted on average signals, fine adaptations can only be observed on subject-specific cases. Thus, Fig. 7

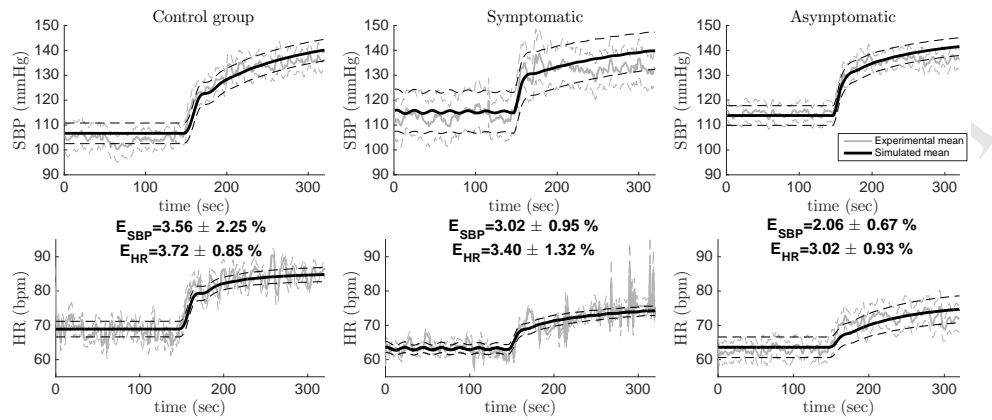


Figure 6: Average fit, and 25% standard deviation, between simulated (black) and experimental (grey) SBP and HR signals for healthy subjects, symptomatic and asymptomatic BS patients.

displays a representative example of fit between the simulated and experimental SBP and HR signals of a healthy subject.

345

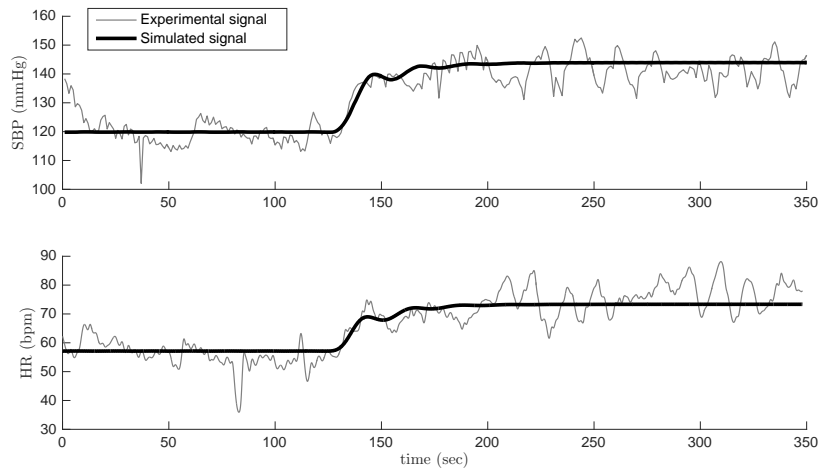


Figure 7: Representative example of fit between simulated (black) and experimental (grey) SBP and HR signals for a healthy subject.

Although some small variations coming from exogenous phenomena, such as temperature, respiration or the central nervous system, could not be simulated

with the proposed model, we observed a significant degree of similarity between experimental and simulated signals; specially during transitory periods, which demonstrates the capability of the model to reproduce HR and SBP responses to HUT testing.

In Fig. 8, boxplots of the identified parameters for the control (C), asymptomatic (A) and symptomatic (S) groups are represented.

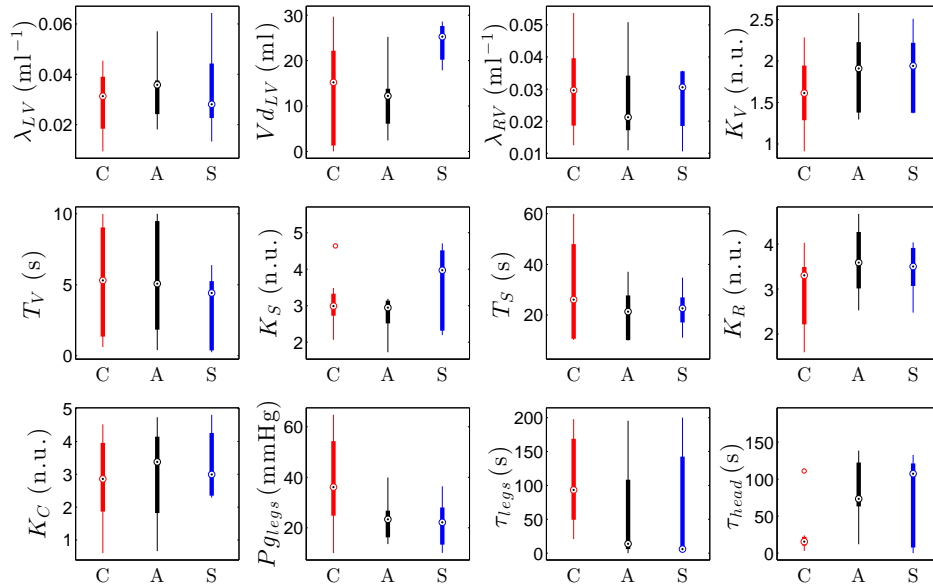


Figure 8: Boxplots of identified parameters; for controls (C), asymptomatic (A) and symptomatic (S) groups.

In addition to identified parameters, the baroreflex response to HUT was also assessed and compared among groups. Fig. 9 displays the mean vagal and sympathetic modulations of the HR for healthy subjects and BS patients, where a greater response with respect to baseline can be observed in controls.

Indeed, ΔS showed a statistically significant reduction in BS patients. Likewise, Vd_{LV} , and thus $V0_{LV}$, were significantly different between symptomatic and asymptomatic patients. Table 3 summarizes the mean \pm standard deviation values for each group, as well as the associated p -values, for these significant

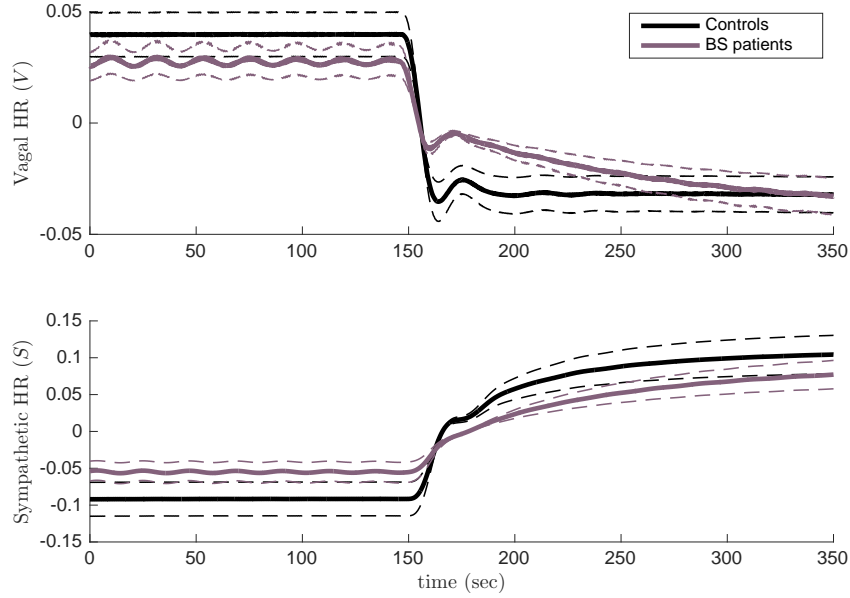


Figure 9: Mean and 25% of standard deviation for the vagal and sympathetic modulations of the HR, resulting from the BRS submodel, for healthy subjects (black) and BS patients (purple). Note that average signals were centered at zero, so as to ease visual comparison between groups.

variables. Supplementary Table IV includes the same information for all analyzed parameters.

Table 3: Mean \pm standard deviation and p -values for statistically significant variables, for a $p < 0.05$ based on Mann-Whitney U tests.

	Controls	BS patients	p-value
	(n=8)	(n=12)	
ΔS	0.19 ± 0.04	0.13 ± 0.06	0.019
	Symptomatic	Asymptomatic	p-value
	(n=5)	(n=7)	
Vd_{LV}	24.00 ± 4.48	11.47 ± 7.46	0.010

4. Discussion

365 This paper proposes a comprehensive model-based analysis of the autonomic
response to HUT on patients suffering from Brugada syndrome. The proposed
model builds up on preliminary work from our team [26], where the feasibility
of the model to reproduce real autonomic responses to HUT testing was already
presented. The main contributions of this paper concern i) the application of
370 a screening sensitivity analysis method allowing for the characterization of the
relative influence of model parameters on the observed HR and SBP responses
and ii) the identification and analysis of subject-specific parameter values that
minimize an error function between the simulated and observed responses. To
our knowledge, these results are original, particularly in the context of BS.

375 Concerning sensitivity analysis, as expected, HR turned to be mostly mod-
ulated by autonomic parameters, whereas SBP was more affected by cardio-
vascular variables coming from the LV. These most relevant parameters found
after sensitivity analysis were then estimated on 20 subjects (8 controls and
12 BS patients), using evolutionary algorithms, so as to design subject-specific
380 instances of the model.

According to subject-specific results captured by Vd_{LV} and $V0_{LV}$, symp-
tomatic patients presented significantly higher values of LV volumes at zero
pressure than asymptomatic patients. This shifts end-systolic and end-diastolic
relationships describing the LV pressure-volume (PV) loop to the right; leading
385 to reduced stroke works (SW), measured as the area enclosed by this PV loop.
Due to higher Vd_{LV} values, the cardiac PV cycle is shortened, suggesting a
decreased inotropism in symptomatic patients. The same effect is observed in
dilated cardiomyopathy, where the LV becomes enlarged without compensatory
thickening of the wall, being unable to pump enough blood to meet the organism
390 metabolic demands.

Although BS patients present no apparent structural cardiopathy, some mi-
croscopic myocardial alterations have been reported, suggesting that the dis-
ease may induce cardiomyopathic changes in some patients [45, 46]. Indeed,

some studies have found significant associations between dilated cardiomyopathy and SCN5A mutations [47, 48], and van Hoorn et al [49] reported that
395 loss-of-function SCN5A mutations in BS seem to be related to ventricular dilatation and impairment in contractile function. Since in our clinical series only three BS patients presented a SCN5A mutation (2 were symptomatic), conclusions on this association between SCN5A mutations and contractile dysfunction
400 cannot be extracted. Nevertheless, these findings provide further evidence for the role of structural myocardial abnormalities in the pathophysiology of BS and encourage the debate on whether the disease should be considered as a genetically mediated functional electrical disorder or rather a cardiomyopathy presenting a significant electrical instability.

405 Furthermore, according to ΔS results, BS patients presented a decreased sympathetic HR modulation difference from baseline in relation to healthy subjects. Results are in line with previous studies where sympathetic dysfunctions have been reported in BS [3, 4, 5]. Moreover, Nakazawa et al [12] analyzed the 24-hour autonomic properties of 27 BS patients and 26 healthy subjects, finding
410 higher vagal and reduced sympathetic tones in symptomatic patients. Similarly, in a previous work where the time-varying autonomic response to a standardized HUT test was assessed in 65 BS patients, symptomatic subjects presented an increased sympathetic modulation during tilting, with respect to baseline, when compared to asymptomatic patients [16]. Similar tendencies were observed in
415 a study where the autonomic response to exercise testing was evaluated on 105 BS patients [15].

Nevertheless, comparisons between controls and BS patients should be interpreted carefully. First, although no statistically significant differences in the mean HR, SBP and BRS in supine position were found between groups, suggesting that reported sympathetic modulation differences do not seem to be
420 related to age (Table 1), the fact that BS patients were significantly older than controls may have a significant impact on autonomic function results. Moreover, although controls were selected after discarding those subjects taking cardioactive medication, they could be treated for non-cardiorespiratory diseases having

425 a significant impact on the autonomic response to HUT testing. Indeed, significant differences in the age of study groups was due to the selection of young healthy volunteers (between 18 and 35 years old) so as to reduce the occurrence of undiagnosed diseases and non-cardiorespiratory medication.

The proposed model and analyses in this work present other limitations that should be mentioned. First, the model can only explain the mechanical, circulatory and autonomic sympathetic functions of the cardiovascular system, ignoring other physiological systems that influence cardiovascular response during HUT. In particular, a respiratory system model should be integrated. Another limitation is related to the fact that the identification process is applied in order to reduce a global error with a unique set of parameters. Some of these parameters may significantly vary during the experimentation, contributing to higher-energy components that are present in the observed signals. A recursive identification process should be performed in the future so as to estimate these time-varying parameter values and better reproduce high-frequency oscillations.

440 Moreover, in order to reduce computational costs during parameter identification, we selected a small sample of variables that may have absorbed changes in other previously fixed parameters. For instance, we found significant results for LV variables that may have been affected by RV variations. Thus, a more exhaustive estimation process including a wider range of variables could be performed in the future. Likewise, since some BS patients were older than those subjects reported in the literature from which physiological ranges were selected for sensitivity analysis, these ranges may be enlarged in the future so as to ensure that the entire age spectrum is being covered. Furthermore, the identified most sensitive parameters may not be representative of the underlying etiology. Thus, the estimation of less sensitive parameters could also provide valuable cardiovascular and autonomic information.

450 Finally, this study is based on a small population of BS patients leading to moderately significant results and, thus, conclusions should be extracted by means of a larger clinical series. Nevertheless, this is the first work comparing healthy subjects and BS patients through a system-level model-based approach.

We consider that the proposed analysis, including cardiovascular parameters never before studied in BS, indicates important trends of clinical relevance that suppose a step forward towards the understanding of the disease.

5. Conclusion

460 This paper presents the integration and analysis of a mathematical model capturing the cardiovascular system dynamics and its autonomic response to head-up tilt testing. First, a parameter sensitivity analysis was applied to identify the most relevant variables affecting blood pressure and heart rate in supine and upright postures. Although sympathetic parameters gained importance
465 during tilting, similar results were obtained for both test phases. Moreover, systolic blood pressure was mainly modulated by cardiovascular parameters, whereas heart rate was mostly affected by autonomic variables.

Then, subject-specific model parameters were estimated by comparing simulated outputs with cardiac experimental data. Results show significant differences
470 between asymptomatic and symptomatic BS patients in the left ventricle volume at zero pressure, suggesting a reduced contractility function in the latter. Moreover, controls showed an increased sympathetic modulation after tilting with respect to BS patients.

Although a more extensive evaluation including a wider range of parameters, a greater number of subjects and the identification of high-frequency oscillations should be performed in the future, this paper presents a first approach
475 towards the evaluation of variables never studied before in BS, thus providing new insights into the underlying autonomic mechanisms regulating the cardiovascular system in this population. The identified parameters might be used as
480 a complementary source of information, along with classical electrophysiological parameters, for BS risk stratification.

Acknowledgements

This work was supported by a grant from the French Ministry of Health (Programme Hospitalier de Recherche Clinique - PHRC Regional); ID RCB 485 2007-A00887-46 and reference 07/28-645. M.C. thanks la Caixa Foundation and D.R. acknowledges Lefoulon-Delalande Foundation for financial support.

References

- [1] S. Priori, C. Blomström-Lundqvist, A. Mazzanti, N. Blom, M. Borggrefe, J. Camm, P. Elliott, D. Fitzsimons, R. Hatala, G. Hindricks, et al., Task 490 force for the management of patients with ventricular arrhythmias and the prevention of sudden cardiac death of the european society of cardiology (esc). 2015 esc guidelines for the management of patients with ventricular arrhythmias and the prevention of sudden cardiac death: the task force for the management of patients with ventricular arrhythmias and the pre- 495 vention of sudden cardiac death of the european society of cardiology (esc) endorsed by: Association for european paediatric and congenital cardiology (aepc), *Europace* 17 (2015) 1601–1687.
- [2] K. Matsuo, T. Kurita, M. Inagaki, M. Kakishita, N. Aihara, W. Shimizu, A. Taguchi, K. Suyama, S. Kamakura, K. Shimomura, The circadian pat- 500 tern of the development of ventricular fibrillation in patients with brugada syndrome, *European heart journal* 20 (6) (1999) 465–470.
- [3] P. Kies, T. Wichter, M. Schäfers, M. Paul, K. P. Schäfers, L. Eckardt, L. Stegger, E. Schulze-Bahr, O. Rimoldi, G. Breithardt, et al., Abnormal myocardial presynaptic norepinephrine recycling in patients with brugada 505 syndrome, *Circulation* 110 (19) (2004) 3017–3022.
- [4] T. Wichter, P. Matheja, L. Eckardt, P. Kies, K. Schäfers, E. Schulze-Bahr, W. Haverkamp, M. Borggrefe, O. Schober, G. Breithardt, et al., Cardiac autonomic dysfunction in brugada syndrome, *Circulation* 105 (6) (2002) 702–706.

- 510 [5] M. Paul, M. Meyborg, P. Boknik, U. Gergs, W. Schmitz, G. Breithardt, T. Wichter, J. Neumann, Autonomic dysfunction in patients with brugada syndrome: further biochemical evidence of altered signaling pathways, *Pacing and Clinical Electrophysiology* 34 (9) (2011) 1147–1153.
- [6] R. Krittayaphong, G. Veerakul, K. Nademane, C. Kangkagate, Heart rate
515 variability in patients with brugada syndrome in thailand, *European Heart Journal* 24 (19) (2003) 1771–1778.
- [7] J.-S. Hermida, A. Leenhardt, B. Cauchemez, I. Denjoy, G. Jarry, F. Mizon, P. Milliez, J.-L. Rey, P. Beaufiles, P. Coumel, Decreased nocturnal standard deviation of averaged nn intervals, *European heart journal* 24 (22) (2003)
520 2061–2069.
- [8] B. Pierre, D. Babuty, P. Poret, C. Giraudeau, O. Marie, P. Cosnay, L. Fauchier, Abnormal nocturnal heart rate variability and qt dynamics in patients with brugada syndrome, *Pacing and clinical electrophysiology* 30 (s1) (2007) S188–S191.
- 525 [9] T. Tokuyama, Y. Nakano, A. Awazu, Y. Uchimura-Makita, M. Fujiwra, Y. Watanabe, A. Sairaku, K. Kajihara, C. Motoda, N. Oda, et al., Deterioration of the circadian variation of heart rate variability in brugada syndrome may contribute to the pathogenesis of ventricular fibrillation, *Journal of cardiology* 64 (2) (2014) 133–138.
- 530 [10] N. Behar, B. Petit, V. Probst, F. Sacher, G. Kervio, J. Mansourati, P. Bru, A. Hernandez, P. Mabo, Heart rate variability and repolarization characteristics in symptomatic and asymptomatic brugada syndrome, *Europace* (2016) euw224.
- [11] A. Kostopoulou, M. Koutelou, G. Theodorakis, A. Theodorakos, E. Livanis,
535 T. Maounis, A. Chaidaroglou, D. Degiannis, V. Voudris, D. Kremastinos, et al., Disorders of the autonomic nervous system in patients with brugada syndrome: a pilot study, *Journal of cardiovascular electrophysiology* 21 (7) (2010) 773–780.

- [12] K. Nakazawa, T. Sakurai, A. Takagi, R. Kishi, K. Osada, T. Nanke,
540 F. Miyake, N. Matsumoto, S. Kobayashi, Autonomic imbalance as a prop-
erty of symptomatic brugada syndrome, *Circulation journal* 67 (6) (2003)
511–514.
- [13] M. Calvo, V. Le Rolle, D. Romero, N. Béhar, P. Gomis, P. Mabo,
A. Hernández, Heart rate differences between symptomatic and asymp-
545 tomatic brugada syndrome patients at night, *Physiological measurement*
39 (6) (2018) 065002.
- [14] M. Calvo, P. Gomis, D. Romero, V. Le Rolle, N. Béhar, P. Mabo,
A. Hernández, Heart rate complexity analysis in brugada syndrome during
physical stress testing, *Physiological measurement* 38 (2) (2017) 387–396.
- 550 [15] M. Calvo, D. Romero, V. Le Rolle, P. Gomis, N. Behar, P. Mabo, A. Her-
nandez, Multivariate classification of brugada syndrome patients based on
autonomic response to exercise testing, *PLoS ONE* 13 (5) (2018) e0197367.
- [16] M. Calvo, V. Le Rolle, D. Romero, N. Béhar, P. Gomis, P. Mabo,
A. Hernández, Time-frequency analysis of the autonomic response to head-
555 up tilt testing in brugada syndrome, in: *Computing in Cardiology Confer-
ence (CinC)*, 2017, 2017.
- [17] M. Calvo, V. Le Rolle, D. Romero, N. Béhar, P. Gomis, P. Mabo,
A. Hernández, Comparison of methods to measure baroreflex sensitivity
in brugada syndrome, in: *Computing in Cardiology Conference (CinC)*,
560 2015, 2015, pp. 245–248.
- [18] V. Le Rolle, A. I. Hernández, P.-Y. Richard, G. Carrault, An autonomic
nervous system model applied to the analysis of orthostatic tests, *Modelling
and Simulation in Engineering* 2008 (2008) 2.
- 565 [19] T. Heldt, E. B. Shim, R. D. Kamm, R. G. Mark, Computational modeling of
cardiovascular response to orthostatic stress, *Journal of applied physiology*
92 (3) (2002) 1239–1254.

- [20] J. J. Smith, *Circulatory response to the upright posture*, no. 6, CRC Press, 1990.
- [21] H. R. Kirchheim, Systemic arterial baroreceptor reflexes, *Physiological Reviews* 56 (1) (1976) 100–177.
- [22] T. F. of the European Society of Cardiology, et al., Heart rate variability standards of measurement, physiological interpretation, and clinical use, *European Heart Journal* 17 (354–381).
- [23] S. Michael, K. S. Graham, G. M. Davis, Cardiac autonomic responses during exercise and post-exercise recovery using heart rate variability and systolic time intervals—a review, *Frontiers in Physiology* 8 (2017) 301.
- [24] A. Malliani, C. Julien, G. E. Billman, S. Cerutti, M. F. Piepoli, L. Bernardi, P. Sleight, M. A. Cohen, C. O. Tan, D. Laude, et al., Cardiovascular variability is/is not an index of autonomic control of circulation, *Journal of Applied Physiology* 101 (2) (2006) 684–688.
- [25] M. Calvo, V. Le Rolle, D. Romero, N. Béhar, P. Gomis, P. Mabo, A. Hernández, Sex-specific analysis of the cardiovascular function, 1st Edition, Springer International Publishing, 2018, Ch. 7b: Gender differences in the autonomic response to exercise testing in Brugada syndrome.
- [26] M. Calvo, V. Le Rolle, D. R. Pérez, N. Béhar, P. Gomis, P. Mabo, A. I. Hernández, Analysis of a cardiovascular model for the study of the autonomic response of brugada syndrome patients, in: 5591-5594 (Ed.), *Engineering in Medicine and Biology Society (EMBC), 2016 IEEE 38th Annual International Conference of the*, 2016.
- [27] H. M. Romero-Ugalde, D. Ojeda, V. L. Rolle, D. Andreu, D. Guiraud, J.-L. Bonnet, C. Henry, N. Karam, A. Hagege, P. Mabo, G. Carrault, A. I. Hernandez, Model-based design and experimental validation of control modules for neuromodulation devices, *Biomedical Engineering, IEEE Transactions on PP* (99) (2015) 1–1.

- 595 [28] A. I. Hernandez, V. Le Rolle, D. Ojeda, P. Baconnier, J. Fontecave-Jallon, F. Guillaud, T. Grosse, R. G. Moss, P. Hannaert, S. R. Thomas, Integration of detailed modules in a core model of body fluid homeostasis and blood pressure regulation, *Prog Biophys Mol Biol* 107 (1) (2011) 169–82.
- [29] V. Le Rolle, D. Ojeda, A. I. Hernández, Embedding a cardiac pulsatile
600 model into an integrated model of the cardiovascular regulation for heart failure followup, *IEEE transactions on biomedical engineering* 58 (10) (2011) 2982–2986.
- [30] D. Ojeda, V. Le Rolle, M. Harmouche, A. Drochon, H. Corbineau, J.-P. Verhoye, A. I. Hernandez, Sensitivity analysis and parameter estimation of
605 a coronary circulation model for triple-vessel disease, *IEEE Transactions on Biomedical Engineering* 61 (4) (2014) 1208–1219.
- [31] A. I. Hernández, V. Le Rolle, A. Defontaine, G. Carrault, A multiformalism and multiresolution modelling environment: application to the cardiovascular system and its regulation, *Philosophical Transactions of the Royal
610 Society of London A: Mathematical, Physical and Engineering Sciences* 367 (1908) (2009) 4923–4940.
- [32] A. I. Hernández, G. Carrault, F. Mora, A. Bardou, Model-based interpretation of cardiac beats by evolutionary algorithms: signal and model interaction, *Artificial Intelligence in Medicine* 26 (3) (2002) 211–235.
- 615 [33] B. W. Smith, J. G. Chase, R. I. Nokes, G. M. Shaw, G. Wake, Minimal haemodynamic system model including ventricular interaction and valve dynamics, *Medical engineering & physics* 26 (2) (2004) 131–139.
- [34] D. Ojeda, V. L. Rolle, K. T. V. Koon, C. Thebault, E. Donal, A. I. Hernández, Towards an atrio-ventricular delay optimization assessed by
620 a computer model for cardiac resynchronization therapy, in: *Proc. SPIE* 8922, IX International Seminar on Medical Information Processing and Analysis, 2013.

- [35] D. Ojeda, V. Le Rolle, O. Rossel, N. Karam, A. Hagege, J.-L. Bonnet, P. Mabo, G. Carrault, A. Hernández, Analysis of a baroreflex model for the study of the chronotropic response to vagal nerve stimulation, in: Neural Engineering (NER), 2015 7th International IEEE/EMBS Conference on, 2015, pp. 541–544.
- [36] M. Ursino, E. Magosso, Acute cardiovascular response to isocapnic hypoxia. i. a mathematical model, *American Journal of Physiology-Heart and Circulatory Physiology* 279 (1) (2000) H149–4165.
- [37] M. D. Morris, Factorial sampling plans for preliminary computational experiments, *Technometrics* 33 (2) (1991) 161–174.
- [38] D. E. Goldberg, J. H. Holland, Genetic algorithms and machine learning, *Machine learning* 3 (2) (1988) 95–99.
- [39] L. Bernardi, G. De Barbieri, M. Rosengård-Bärlund, V.-P. Mäkinen, C. Porta, P.-H. Groop, New method to measure and improve consistency of baroreflex sensitivity values, *Clinical Autonomic Research* 20 (6) (2010) 353–361.
- [40] R. B. Leman, E. Clarke, P. GILLETTE, Significant complications can occur with ischemic heart disease and tilt table testing, *Pacing and clinical electrophysiology* 22 (4) (1999) 675–677.
- [41] R. Sheldon, S. Rose, M. L. Koshman, Isoproterenol tilt-table testing in patients with syncope and structural heart disease., *The American journal of cardiology* 78 (6) (1996) 700–703.
- [42] P. H. Kim, S. J. Ahn, J. S. Kim, Frequency of arrhythmic events during head-up tilt testing in patients with suspected neurocardiogenic syncope or presyncope, *The American journal of cardiology* 94 (12) (2004) 1491–1495.
- [43] J. Shenthara, D. Pujar, M. A. Prabhu, P. S. Surhynne, Ventricular fibrillation a rare complication during head-up tilt test, *HeartRhythm case reports* 1 (5) (2015) 363.

- [44] J. Dumont, A. I. Hernandez, G. Carrault, Improving ecg beats delineation with an evolutionary optimization process, *IEEE Transactions on Biomedical Engineering* 57 (3) (2010) 607–615.
- [45] A. Frustaci, S. G. Priori, M. Pieroni, C. Chimenti, C. Napolitano, I. Rivolta, T. Sanna, F. Bellocci, M. A. Russo, Cardiac histological substrate in patients with clinical phenotype of brugada syndrome, *Circulation* 112 (24) (2005) 3680–3687.
- [46] A. Frustaci, M. A. Russo, C. Chimenti, Structural myocardial abnormalities in asymptomatic family members with brugada syndrome and scn5a gene mutation, *European Heart Journal* 30 (14) (2009) 11763.
- [47] W. P. McNair, L. Ku, M. R. Taylor, P. R. Fain, D. Dao, E. Wolfel, L. Mestroni, , Scn5a mutation associated with dilated cardiomyopathy, conduction disorder, and arrhythmia, *Circulation* 110 (15) (2004) 2163–2167.
- [48] W. P. McNair, G. Sinagra, M. R. Taylor, A. D. Lenarda, D. A. Ferguson, E. E. Salcedo, D. Slavov, X. Zhu, J. H. Caldwell, L. Mestroni, Scn5a mutations associate with arrhythmic dilated cardiomyopathy and commonly localize to the voltage-sensing mechanism, *Journal of the American College of Cardiology* 57 (21) (2011) 2160 – 2168.
- [49] F. van Hoorn, M. E. Campian, A. Spijkerboer, M. T. Blom, R. N. Planken, A. C. van Rossum, J. M. T. de Bakker, A. A. M. Wilde, M. Groenink, H. L. Tan, Scn5a mutations in brugada syndrome are associated with increased cardiac dimensions and reduced contractility, *PLoS One* 7 (8) (2012) e42037.

- Blood pressure is mainly influenced by cardiovascular parameters.
- Heart rate is mostly modulated by baroreflex regulation.
- Brugada syndrome patients show a decreased sympathetic modulation after tilting.
- A reduced left ventricular contractility is observed in symptomatic patients.

ACCEPTED MANUSCRIPT